



Published in final edited form as:

*Free Radic Biol Med.* 2015 September ; 86: 25–36. doi:10.1016/j.freeradbiomed.2015.04.009.

## **Sigma 1 Receptor regulates the oxidative stress response in primary retinal Müller glial cells via Nrf2 signaling and system $x_c^-$ , the $Na^+$ -independent glutamate-cystine exchanger**

**J. Wang<sup>1,2</sup>, A. Shanmugam<sup>1,2</sup>, S. Markand<sup>1,2</sup>, E. Zorrilla<sup>3</sup>, V. Ganapathy<sup>2,4</sup>, and S.B. Smith<sup>1,2,5</sup>**

<sup>1</sup>Department of Cellular Biology and Anatomy, Medical College of Georgia, Georgia Regents University, Augusta, GA

<sup>2</sup>James and Jean Culver Vision Discovery Institute, Georgia Regents University, Augusta, GA

<sup>3</sup>Harold L. Dorris Neurological Research Institute, The Scripps Research Institute, La Jolla, CA

<sup>4</sup>Department of Biochemistry and Molecular Biology, Medical College of Georgia, Georgia Regents University, Augusta, GA

<sup>5</sup>Department of Ophthalmology, Medical College of Georgia, Georgia Regents University, Augusta, GA

### **Abstract**

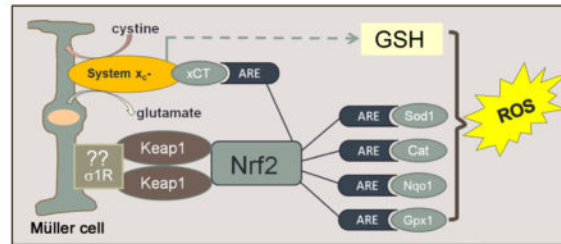
Oxidative stress figures prominently in retinal diseases including diabetic retinopathy and glaucoma. Ligands for  $\sigma$ 1R, a unique transmembrane protein localized to the ER, mitochondria, nuclear and plasma membrane, have profound retinal neuroprotective properties *in vitro* and *in vivo*. Studies to determine the mechanism of  $\sigma$ 1R-mediated retinal neuroprotection have focused mainly on neurons. Little is known about effects of  $\sigma$ 1R on Müller cell function, yet these radial glial cells are essential for homeostatic support of the retina. Here we investigated whether  $\sigma$ 1R mediates the oxidative stress response of Müller cells using wildtype (WT) and  $\sigma$ 1R knockout ( $\sigma$ 1RKO) mice. We observed increased endogenous ROS levels in  $\sigma$ 1RKO Müller cells compared to WT, which was accompanied by decreased expression of *Sod1*, *Catalase*, *Nqo1*, *Hmox1*, *Gstm6* and *Gpx1*. The protein levels of SOD1, CAT, NQO1 and GPX1 were also significantly decreased. The genes encoding these antioxidants contain an antioxidant response element (ARE), which under stress is activated by NRF2, a transcription factor that typically resides in the cytoplasm bound by KEAP1. In the  $\sigma$ 1RKO Müller cells *Nrf2* expression was decreased significantly at the gene (and protein) level, while *Keap1* gene (and protein) levels were markedly increased. NRF2-ARE binding affinity was decreased markedly in  $\sigma$ 1RKO Müller cells. We investigated system  $x_c^-$ , the cystine-glutamate exchanger important for synthesis of GSH, and observed decreased

\*Please send correspondence to: Sylvia B. Smith, Ph.D., Department of Cellular Biology and Anatomy, Medical College of Georgia, Georgia Regents University, 1120 15<sup>th</sup> Street, CB 1114, Augusta, GA 30912-2000, 706-721-7392 (phone), 706-721-6120 (fax), sbsmith@gru.edu.

**Publisher's Disclaimer:** This is a PDF file of an unedited manuscript that has been accepted for publication. As a service to our customers we are providing this early version of the manuscript. The manuscript will undergo copyediting, typesetting, and review of the resulting proof before it is published in its final citable form. Please note that during the production process errors may be discovered which could affect the content, and all legal disclaimers that apply to the journal pertain.

function in  $\sigma 1$ RKO Müller cells compared to WT as well as decreased GSH and GSH/GSSG ratios. This was accompanied by decreased gene and protein levels of xCT, the unique component of system  $x_c^-$ . We conclude that Müller glial cells lacking  $\sigma 1$ R manifest elevated ROS, perturbation of antioxidant balance, suppression of NRF2 signaling and impaired function of system  $x_c^-$ . The data suggest that the oxidative stress-mediating function of retinal Müller glial cells may be compromised in the absence of  $\sigma 1$ R. The neuroprotective role of  $\sigma 1$ R may be linked directly to the oxidative stress-mediating properties of supportive glial cells.

## Graphical abstract



Schematic of paper: Oxidative stress in the form of reactive oxygen species (ROS) figures prominently in retinal diseases. The Müller glial cell is a major mediator of retinal homeostasis. In this paper, Müller cells harvested from mice lacking  $\sigma 1$ R, a putative molecular chaperone, showed an increase endogenous production of ROS. This was accompanied by decreased expression of a number of antioxidant proteins, which are known to harbor antioxidant response elements (ARE). Nrf2, which is a major regulator of oxidative stress through its activation of AREs was decreased at the gene, protein and activity level; its major regulatory protein Keap1 was increased. The expression and activity of the cystine-glutamate exchanger was also decreased in Müller cells lacking  $\sigma 1$ R. Taken collectively, the data support a key role for  $\sigma 1$ R in modulation of oxidative stress in retina.

## Keywords

retina; retinal Müller glial cells; sigma 1 receptor ( $\sigma 1$ R); system  $x_c^-$ ; xCT; Nrf2; mouse

## Introduction

Oxidative stress is implicated in a number of devastating neurodegenerative diseases including those of the retina such as age-related macular degeneration, glaucoma, diabetic retinopathy and retinitis pigmentosa. While the underlying causes of these retinopathies vary, oxidative stress, activation of pro-apoptotic pathways and increased ER stress are features common to all of these diseases [1,2]. Sigma-1 receptor ( $\sigma 1$ R) has emerged as a promising target for treatment of neurodegenerative diseases owing to its role in cellular survival [3].  $\sigma 1$ R is a unique 223-amino acid integral membrane protein that spans the membrane twice and also has a third membrane flanking domain [4]. It has been cloned in guinea pig, mouse and human [5–7].  $\sigma 1$ R shares no homology with any other mammalian receptor systems. The hallucinogen N,N-dimethyltryptamine was reported as an endogenous agonist for  $\sigma 1$ R [8], but no other natural ligands have been identified.

$\sigma$ 1R appears to play key roles in a number of critical cellular functions. For example, ligands for  $\sigma$ 1R can prevent apoptotic cell death in brain-derived neuronal cultures [9–11] as well as in retinal neurons *in vitro* and *in vivo* [12–15]. It has been postulated that  $\sigma$ 1R functions as a ligand-operated chaperone in complex with the master endoplasmic reticulum (ER) regulatory protein, BiP [16]. ER stress is inexorably linked to oxidative stress. As Malhotra and Kaufman [17] review, the ER is a “protein-folding machine” composed of chaperone proteins, proteins that catalyze protein folding, and sensors that detect the presence of misfolded or unfolded proteins. The ER provides a unique oxidizing folding-environment that favors the formation of the disulfide bonds; protein folding and generation of reactive oxygen species (ROS) as a byproduct of protein oxidation in the ER are closely linked.  $\sigma$ 1R can stabilize the inositol 1,4,5-triphosphate type 3 receptor and its ligands modulate ER stress in a variety of cellular systems including retina [16, 18–25]. Of particular interest for the current study are reports that ligands for  $\sigma$ 1R can suppress production of reactive oxygen species (ROS) in many tissue types including lung, liver [26], cultured lens cells [18], retinal pigment epithelial cells [27] and retinal neurons [25].

The mechanism by which  $\sigma$ 1R modulates oxidative stress was investigated recently in lung and liver using mice that lack  $\sigma$ 1R ( $\sigma$ 1R knockout (KO) mice) [26]. Metabolomics studies showed an increase in oxidative stress markers (including oxidized glutathione (GSSG) and glutamate) in lung and liver of  $\sigma$ 1RKO mice compared to wild type (WT) mice. In that same study, COS-7 cells, which were transfected with  $\sigma$ 1R, demonstrated an activation of antioxidant response elements (ARE) in the presence of ligands for  $\sigma$ 1R. *Sigma1r*-transfected cells upregulated genes encoding two important antioxidant proteins, NAD(P)H quinone oxidoreductase (NQO1) and superoxide dismutase (SOD-1) when they were treated with  $\sigma$ 1R ligands. These findings are relevant to retinal disease because ligand binding activity to  $\sigma$ 1R increases in retina, specifically in retinal Müller glial cells, following exposure to donors of nitric oxide and ROS [28].

The current study examined the role of  $\sigma$ 1R in modulating oxidative stress in retinal Müller cells, the major glial cell of the retina. Müller cells are radial macroglial cells offering stability to the complex retinal architecture and providing support for the function and metabolism of retinal neurons and blood vessels [29]. Müller cells play a key role in normal retinal function and become activated in response to pathological stimuli. They hypertrophy and proliferate under pathologic conditions leading to formation of glial scars, which fill the spaces left by dying neurons and dysfunctional synapses. Understanding the role of  $\sigma$ 1R in these sustentacular cells may facilitate development of novel neuroprotective approaches for oxidative stress-induced retinal disease. In this study we report elevated endogenous ROS levels and reduced glutathione (GSH) levels in Müller cells harvested from  $\sigma$ 1RKO mice compared to WT. We also observed decreased expression of several antioxidant genes leading to investigation of the nuclear factor erythroid-2 related factor (NRF2)-Kelch like-ECH-associated protein 1 (KEAP1) pathway, which was markedly perturbed in glial cells lacking  $\sigma$ 1R. We investigated also the activity of the cystine-glutamate exchanger, system  $x_c^-$ , because of its role in synthesis of GSH [30,31] and found significantly reduced activity in  $\sigma$ 1RKO cells. Our data provide strong evidence that  $\sigma$ 1R regulates oxidative stress through modulation of the NRF2-KEAP1 pathway as well as system  $x_c^-$ .

The findings of the present study are not only important with respect to blinding retinal diseases, which exact a devastating toll on quality of life, but also to cancer, cardiovascular diseases, and neurodegenerative diseases because oxidative stress is overwhelmingly implicated in their pathogenesis [32]. While the current studies focused on a specific cell type within retina, the findings have far-reaching implications with respect to  $\sigma$ 1R function and support the notion that  $\sigma$ 1R is a modulator of oxidative stress in multiple tissue types including liver, brain, lung [16, 23, 26] and retina [25]. Our findings that absence of  $\sigma$ 1R may be linked to alterations in expression of the Nrf2-Keap1 pathway are novel and highly significant. The expression and activity of Nrf2 are decreased significantly in retinal Müller glial cells lacking  $\sigma$ 1R. Nrf2 is arguably the most important regulator of the expression of antioxidant molecules [33], thus this first report that lack of  $\sigma$ 1R is linked to decreased Nrf2 levels could provide important clues to the mechanism by which  $\sigma$ 1R acts as a mediator of oxidative stress as well as to the mechanism by which some of its ligands mediate cellular protection.

## Materials and methods

### Isolation of primary mouse Müller cells

Wildtype ( $\sigma$ 1R<sup>+/+</sup>, WT) and  $\sigma$ 1R knockout ( $\sigma$ 1R<sup>-/-</sup>,  $\sigma$ 1RKO) mice were used for isolation of Müller cells. The  $\sigma$ RI<sup>-/-</sup> mice were generated by gene trapping (Opr1<sup>Gt(IRESBetageo)33Lex</sup>/Opr1<sup>Gt(IRESBetageo)33Lex</sup>) conducted at Lexicon Genetics Corp. (The Woodlands, TX; [http://www.informatics.jax.org/searches/accession\\_report.cgi?id=MGI:3529055](http://www.informatics.jax.org/searches/accession_report.cgi?id=MGI:3529055)). Heterozygote Opr1 mutant (+/-) Opr1<sup>Gt(IRESBetageo)33Lex</sup> embryos on a C57BL/6J × 129S/SvEv mixed background were obtained from the Mutant Mouse Resource Regional Center and implanted into female C57BL/6J mice (Jackson Laboratories, Bar Harbor, ME) at The Scripps Research Institute as reported [34]. Founder heterozygous mice were transferred to the animal facility at Georgia Regents University, and colonies of wild-type ( $\sigma$ RI<sup>+/+</sup>), heterozygous ( $\sigma$ RI<sup>+/-</sup>), and homozygous ( $\sigma$ RI<sup>-/-</sup>) mice were established. Genotyping of mice followed our published protocol [35]. Maintenance of animals adhered to institutional guidelines for the humane treatment of animals and to the ARVO Statement for the Use of Animals in Ophthalmic and Vision Research ([http://www.arvo.org/About\\_ARVO/Policies/Statement\\_for\\_the\\_Use\\_of\\_Animals\\_in\\_Ophthalmic\\_and\\_Visual\\_Research](http://www.arvo.org/About_ARVO/Policies/Statement_for_the_Use_of_Animals_in_Ophthalmic_and_Visual_Research)). Müller cells were isolated from 5~7-day-old pups and cultured per our method [36] based upon the original report by Hicks and Cortois [37]. Briefly, eyeballs were removed, placed in serum-free Dulbecco's modified Eagle medium (DMEM) with penicillin/streptomycin and soaked overnight at 25 °C in the dark. They were rinsed in phosphate-buffered saline (PBS) and incubated in buffer containing trypsin, EDTA and collagenase. Retinas were removed from eyeballs, placed in DMEM supplemented with glucose, fetal bovine serum and penicillin/streptomycin and gently pipetted into small aggregates. Cultures were washed vigorously with medium until only a strongly adherent, flat, cell population remained. Cells were used at passage 4–5. The purity of cultures has been verified in earlier studies [28, 36] in which antibodies that are known markers of Müller cells were used: cellular retinaldehyde binding protein (CRALBP) (Laboratory of Dr. J Saari, U. Washington), vimentin (Millipore, Billerica, MA, Cat. No: AB-1620), glutamine synthetase (Santa Cruz Corp., Santa Cruz,

CA, Cat. No. SC- C20), glutamate-aspartate transporter ((GLAST), Alpha Diagnostics, San Antonio, TX, Cat. No: 11-S)). Earlier studies used immunocytochemical analysis of markers for neurons (NF-L (neurofilament-light), SC-H70), a major component of neuronal cytoskeleton), retinal pigment epithelial protein 65 (RPE-65, gift from Dr. M. Redmond, NEI, NIH) and microglial cells (ionized calcium binding adaptor molecule 1 (IBA1, #019-19741, Wako Chemicals, Richmond, VA)) and showed minimal detection in cultures [28, 36].

### Immunocytochemical confirmation of $\sigma$ R1 in retinal Müller cells

Müller cells from WT and  $\sigma$ 1RKO mice were seeded on coverslips, grown for 24 h, fixed with ice-cold 4% paraformaldehyde (PFA, Electron Microscopy Science, Hatfield, PA), washed with PBS-Triton X-100, incubated with Power Block, (BioGenex, Fremont, CA) and then incubated overnight at 4°C with rabbit polyclonal  $\sigma$ R1 (1:1000) [38] or with goat polyclonal anti-vimentin (1:200) antibody. Cells were washed thrice with PBS-Triton X-100 followed by incubation with secondary antibodies (goat anti-rabbit IgG coupled to Alexa Fluor 568 and donkey anti-goat IgG coupled to Alexa Fluor 488 (1:1000) for 1 h at 37 °C. Cells were washed with PBS-Triton X-100 and coverslipped with Fluoroshield with DAPI (Sigma-Aldrich, St. Louis, MO) to label nuclei. Negative controls were treated identically except that PBS replaced the primary antibodies. Immunofluorescent signals were visualized using an Axioplan-2 fluorescent microscope (Carl Zeiss, Göttingen, Germany) equipped with an HRM camera. Images were captured and processed using Zeiss Axiovision digital image processing software (version 4.7).

### ROS detection

Müller cells harvested from WT and  $\sigma$ 1RKO mice were seeded on coverslips. They were exposed to media containing hydrogen peroxide ( $H_2O_2$ , 200 $\mu$ M) for 6 h. In companion studies, cells were pre-treated 30 min with (+)-pentazocine ((+)-PTZ, 10 $\mu$ M, Sigma-Aldrich, St. Louis, MO, Cat. No: P-127), a high affinity  $\sigma$ 1R ligand, alone or were exposed to  $H_2O_2$  plus (+)-PTZ for 6 h. Control experiments were conducted in parallel in which  $H_2O_2$  and (+)-PTZ were omitted from the media. At the end of the 6 h, cells were rinsed with PBS so that exogenous  $H_2O_2$  was removed. Intracellular ROS was detected in cells using 5  $\mu$ M CellROX Green Reagent (Molecular Probes, Life Technologies, NY, NY; 30 min incubation, followed by fixation). CellROX detects hydroxyl, peroxy, peroxynitrite and hydroxyl radicals. DAPI was used to stain nuclei. Green fluorescent signals representing ROS were visualized using an Axioplan-2 fluorescent microscope (described above). Fluorescence intensity was quantified using Image J 1.48v software (National Institutes of Health, Bethesda, MD, USA).

To quantify endogenous ROS in WT and  $\sigma$ 1RKO Müller cells, cells were seeded in a black-sided, clear-bottomed 24-well plate ( $5 \times 10^4$  cells per well) overnight. Cell culture media was removed by aspiration. Certain wells of WT and  $\sigma$ 1RKO Müller cells were used for protein determination, while the remaining wells were rinsed twice with warm (37°C) HBSS, were then incubated with 20  $\mu$ M 6-carboxy-2',7'-dichlorodihydrofluorescein diacetate (carboxy-H2DCFDA) (C-400, Molecular Probes) in HBSS (1h, 37°C) in the dark according to the method of Tetz [39]. This probe measures formation of ROS such as peroxynitrite,

hydroxide radicals, and molecules that include peroxy, alkoxy, carbonate ( $\text{CO}_3^-$ ) and  $\text{NO}_2\cdot$  groups. Fluorescence readings of carboxy-DCFH-DA (495 nm excitation and 527 nm emission) of WT and  $\sigma$ 1RKO Müller cells were taken at 1 h intervals for 6 h at 37°C using a Synergy H1 Hybrid multi-mode microplate reader (BioTek, Winooski, VT, USA). The fluorescence of carboxy-H2DCFDA without any samples was taken as the blank. Results were shown as fluorescence (arbitrary units) per  $\mu\text{g}$  cell lysate in  $\sigma$ 1RKO mice compared to WT Müller cells.

### Quantitative real-time RT-PCR

Expression levels of mRNA transcripts specific for several key genes (*Sod1*, *Cat*, *Nqo1*, *Hmox1*, *Gstm3*, *Gstm6*, *Gstt3*, *Gpx1*, *Gpx2*, *Gpx3*, *Nrf2*, *Keap1* and *xCT*) involved in the antioxidant response, the NRF2 pathway and system  $x_c^-$  were examined in WT and  $\sigma$ 1RKO Müller cells. Total RNA was purified using Trizol (Invitrogen, Carlsbad, CA, USA) according to the manufacturer's protocol and quantified. RNA (2  $\mu\text{g}$ ) was reverse-transcribed using the iScript Synthesis kit (BioRad Laboratories, Hercules, Calif., USA). cDNAs were amplified for 40 cycles by using SsoAdvanced™ SYBR Green Supermix (BioRad Laboratories) and gene-specific primers (Table 1) in a CFX96 Touch™ Real-Time PCR Detection System (BioRad Laboratories). Expression levels were calculated by comparison of Ct values (delta-delta Ct) [25].

### Western blot analysis of antioxidant proteins

Protein was extracted from Müller cells and neural retina isolated from WT and  $\sigma$ 1RKO mice per our method [20]. Proteins were subjected to SDS-polyacrylamide gel electrophoresis. Immunoblotting was performed to assess the levels of the following proteins:  $\sigma$ 1R, SOD1, Catalase, NQO1, HMOX-1, GPX1, GPX2, NRF2, KEAP1, xCT and GAPDH. Nitrocellulose membranes to which the proteins had been transferred were incubated with primary antibodies at the concentrations listed in Table 2. They were incubated with horseradish-peroxidase-conjugated goat anti-rabbit or goat anti-mouse IgG antibody (Santa Cruz Corp., Santa Cruz, CA, USA). Proteins were visualized by using the SuperSignalWest Pico Chemiluminescent Substrate detection system (Pierce Biotechnology, Rockford, Ill., USA). All western blotting images are representative of three or more independent experiments. The bands from western blotting were quantified using the Image J 1.48v software.

### Immunofluorescent detection of NRF2 and KEAP1

Müller cells harvested WT and  $\sigma$ 1R KO mice were seeded on coverslips, grown for 24 h, fixed with ice-cold 4% PFA, washed with PBS-Triton X-100, incubated with Power Block and incubated overnight at 4°C with antibodies against NRF2 and KEAP1 (vendors and concentrations provided in Table 2). The cells were washed three times with PBS-Triton X-100 followed by incubation with secondary antibodies (goat anti-rabbit IgG coupled to Alexa Fluor 568 and goat anti-rabbit IgG coupled to Alexa Fluor 488 (1:1000)) for 1 h at 37°C. Cells were washed with PBS-Triton X-100 three times and coverslipped with Fluoroshield with DAPI (Sigma-Aldrich) to label nuclei. Negative controls were treated



identically except that PBS replaced the primary antibodies. Microscopic detection was performed using the Axioplan-2 fluorescent microscope as described above.

### Analysis of NRF2 binding activity with ARE by trans-activation assay

NRF2 activation and antioxidant response element (ARE) binding efficacy in WT and  $\sigma$ 1RKO Müller cells were evaluated in nuclear extracts using a TransAM<sup>®</sup> NRF2 Kit (50296, Active Motif, Carlsbad, CA). 5, 10, 20 and 40- $\mu$ g aliquot of nuclear protein were incubated with immobilized oligonucleotides containing the ARE consensus binding site (5'-GTC ACA GTA CTC AGC AGA ATC TG-3'), separately. The active form of NRF2 that bound to the oligonucleotides was detected using anti-NRF2 primary antibody followed by incubation with HRP-conjugated secondary antibody. The activity of NRF2 in the nuclear extracts, demonstrated by DNA binding activity of NRF2, was measured by colorimetric detection using a VersaMax microplate reader (Molecular Devices, Sunnyvale CA) at 450 nm; absorbance values reflected the activity of NRF2.

### Functional assay to determine transport activity and kinetics of system $x_c^-$

Uptake of glutamate by the  $\text{Na}^+$ -independent system  $x_c^-$  was performed in cultured Müller cells using an uptake buffer containing: 25 mM 4-(2-hydroxyethyl)-1-piperazineethansulfonic acid (HEPES)/Tris, 140 mM *N*-methyl-D-glucamine chloride, 5.4 mM KCl, 1.8 mM  $\text{CaCl}_2$ , 0.8 mM  $\text{MgSO}_4$ , and 5 mM glucose, pH 7.5. System  $x_c^-$  is a freely reversible exchanger for cystine and glutamate; its transport function can be studied by monitoring the influx of radiolabeled cystine in exchange for the efflux of cellular glutamate or by monitoring either the influx or efflux of radiolabeled glutamate (since system  $x_c^-$  can also function as a  $\text{Na}^+$ -independent glutamate/glutamate exchanger). (Note that once inside the cell, cystine is converted to cysteine, which is not transported by system  $x_c^-$ .) The intracellular level of cystine is necessarily low and hence would not be an easily measured substrate for the transporter. The most accurate method to study the transporter function is to measure influx of [<sup>3</sup>H]-labeled substrate, rather than the highly unstable [<sup>35</sup>S]-labeled cystine. Even though  $\text{Na}^+$ -independent glutamate uptake can occur via AGT1 (alpha-glucoside transporter), there is no evidence for expression of this transporter in the retina [40], thus  $\text{Na}^+$ -independent uptake of glutamate in Müller cells represents the function of system  $x_c^-$  exclusively [41]. L-[G-<sup>3</sup>H]-glutamic acid (specific radioactivity 27.0 Ci/mmol, concentration 1.0 mCi/ml, Moravek Biochemicals and Radiochemicals, Brea, CA) was used as the substrate for uptake experiments. Uptake was initiated by adding 250  $\mu$ l of uptake buffer containing 2.5  $\mu$ M glutamate spiked with 4.0  $\mu$ Ci/ml of radiolabeled [<sup>3</sup>H]-glutamate. Müller cells were incubated for 15 min at 37°C, after which, buffer was removed and cells were washed twice with ice-cold uptake buffer (to stop uptake). The cells were solubilized with 0.5 ml of 1% sodium dodecyl sulfate-0.2N NaOH (SDS/NaOH) and radioactivity was determined by liquid scintillation spectrometry (Beckman LS 6500 scintillation counter, Beckman Instruments, Brea CA). Protein was measured using the Bio-Rad protein assay reagent. Uptake by system  $x_c^-$  was calculated directly from the radioactivity (cpm) data and expressed as pmol/mg protein/15 min.

Kinetic analysis of system  $x_c^-$  was performed in Müller cells harvested from WT and  $\sigma$ 1RKO mice and activity was assessed using increasing amounts of cold glutamate as a

competitor ranging from 2.5  $\mu\text{M}$  to 1000  $\mu\text{M}$ . SigmaPlot 2002 for Windows XP Professional (SPSS Inc., Chicago, IL) was used to calculate  $K_m$  and  $V_{max}$  from an Eadie-Hofstee plot of  $V$ , uptake velocity (pmol/mg protein/15 min) versus  $V/S$  where  $S$  is cold glutamate concentration ( $\mu\text{M}$ ). The formula underlying the Eadie-Hofstee plot is  $v = K_m v/[S] + V_{max}$  where  $v$  represents reaction velocity,  $K_m$  is the Michaelis-Menten constant,  $[S]$  is the substrate concentration, and  $V_{max}$  is the maximum reaction velocity. Experiments were repeated three times; results are expressed as the mean  $\pm$  SE.

### Assessment of intracellular GSH levels

To estimate levels of GSH in Müller cells harvested from WT and  $\sigma 1\text{RKO}$  mice, CellTracker™ Green CMFDA dye (5-Chloromethylfluorescein Diacetate) (Molecular Probes®, Life technologies, NY, USA) was used. Cells were incubated with 1  $\mu\text{M}$  CMFDA at 37°C for 40 min, incubated with fresh pre-warmed medium for 30 min followed by fixation with ice-cold 4% PFA. Nuclei were stained with DAPI. Fluorescence detection was performed using the Axioplan-2 fluorescent microscope as described above. Fluorescence intensity was quantified using Image J 1.48v software. To verify these findings directly, cellular GSH levels per protein and glutathione redox state (GSH/GSSG) were determined using the Glutathione (GSSG/GSH) Detection Kit (ADI-900–160, Enzo Life Sciences, Farmingdale, NY) according to the manufacturer's instructions. WT and  $\sigma 1\text{RKO}$  Müller cells were harvested and a small aliquot of the cell suspension was used for protein determination; the remaining samples were treated with 5% (w/v) MPA (Metaphosphoric acid, Cat. No.239275, Sigma Chem. Corp.) to precipitate proteins, which interfere with the assay. A known volume of the MPA extract was treated without (for total GSH) or with 4-vinylpyridine (only for GSSG analysis), and appropriate GSSG standards were treated similarly to prepare a standard curve. After adding appropriate volumes of freshly-prepared reaction mix (glutathione reductase with reaction mix buffer), a kinetic GSH-reductase recycling assay was performed following the manufacturer's instruction using a VersaMax microplate reader (Molecular Devices, Sunnyvale CA) set at 405nm and read at 1min intervals over a 15 min time period).

### Statistical analysis

Data (with the exception of system  $x_c^-$  kinetic analysis) were analyzed by one- or two-way analysis of variance (ANOVA) as appropriate; Tukey HSD was the post-hoc test. Statistical analyses were conducted using the GraphPad Prism analytical program (LaJolla, Calif., USA). A p value  $<0.05$  was considered significant.

## Results

### Detection of $\sigma 1\text{R}$ in retinal Müller glial cells

Immunofluorescent detection for vimentin was positive in Müller cells harvested from WT and  $\sigma 1\text{RKO}$  mice confirming the glial origin of the cells (Fig. 1A). Immunocytochemical analysis confirmed that  $\sigma 1\text{R}$  is expressed in WT Müller cells but is not present in Müller cells isolated from  $\sigma 1\text{RKO}$  mice (Fig. 1A). The labeling observed (primarily in the nuclear membrane and the perinuclear region) is consistent with an earlier report that  $\sigma 1\text{R}$  is present in the nuclear and ER membranes [28]. Western blot analysis of proteins isolated from WT



cells using an antibody specific for  $\sigma$ 1R yielded a band of the expected size ( $M_r$  25–27 kD) corresponding to  $\sigma$ 1R.  $\sigma$ 1R was not detected in  $\sigma$ 1RKO Müller cells. Equivalent amounts of protein were loaded on the gels as detected by GAPDH (Fig. 1B). The data verify that  $\sigma$ 1R is not present in Müller cells of the  $\sigma$ 1RKO mouse and thus provide a powerful tool to evaluate the role of  $\sigma$ 1R in modulating oxidative stress.

### Elevated endogenous ROS in $\sigma$ 1RKO Müller cells compared to WT

In our initial studies of oxidative stress, WT and  $\sigma$ 1RKO Müller cells were treated with  $H_2O_2$ , subsequently ROS levels were detected using CellROX reagent followed by immunofluorescence detection. Experiments were conducted using  $H_2O_2$  in the presence (or absence) of the  $\sigma$ 1R ligand (+)-PTZ. In the WT cells, there was very little ROS detected in control (non-treated cells) and (+)-PTZ treated cells, but a significant increase in cells exposed to  $H_2O_2$  (Fig. 2A).  $H_2O_2$ -exposed cells treated with (+)-PTZ showed a marked decrease in ROS production compared to  $H_2O_2$ -exposed cells that did not receive (+)-PTZ treatment suggesting that activation of  $\sigma$ 1R attenuates oxidative stress in Müller cells (Fig. 2A). The same experiments conducted with  $\sigma$ 1RKO Müller cells yielded intriguing results. First, as anticipated there was a significant increase in ROS in the  $H_2O_2$ -exposed  $\sigma$ 1RKO cells compared to WT control cells. Second, there was no attenuation of ROS in the presence of the  $\sigma$ 1R ligand (+)-PTZ, a result predicted because the cells do not express  $\sigma$ 1R and previous studies showed that the receptor is required for neuroprotective effects of (+)-PTZ [42,43]. The surprising result was that there was a significantly greater level of ROS detected in  $\sigma$ 1RKO cells that had received no treatment (i.e. control, no  $H_2O_2$  or (+)-PTZ) compared to control WT cells. That is, using the CellROX® Green Reagent detection assay, we observed significantly higher endogenous levels of ROS in cells lacking  $\sigma$ 1R compared to  $\sigma$ 1R expressing cells (Fig. 2B). The data from this experiment were quantified as fluorescent intensity. The ROS levels in Müller cells from  $\sigma$ 1RKO mice were significantly increased (nearly two-fold) compared to WT (Fig. 2C). We confirmed the observation that basal ROS levels in  $\sigma$ 1RKO Müller cells are significantly higher than WT by measuring ROS quantitatively (e.g. measuring the oxidative conversion of carboxyl-DCFH-DA to the highly fluorescent carboxyl-DCF). We observed a significant increase in ROS in  $\sigma$ 1RKO Müller cells compared to WT (Fig. 2D). These data led us to investigate oxidative stress mediators in  $\sigma$ 1RKO Müller cells compared to WT.

### Perturbation of antioxidant balance in $\sigma$ 1RKO Müller glia

We asked whether  $\sigma$ 1R is involved in regulating antioxidant balance by examining the expression of genes encoding antioxidant proteins including SOD1, catalase (CAT), NQO1, hemoxygenase-1 (HMOX1), glutathione-S-transferases (GST) (including GSTm3, GSTm6, GSTT3), and glutathione peroxidases (GPX1, GPX2, GPX3) using  $\sigma$ 1RKO and WT Müller cells. qRT-PCR analysis showed that the expression of several genes was decreased significantly in  $\sigma$ 1RKO Müller cells compared to WT (Fig. 3A), i.e. *Sod1* (decreased by ~65%), *Cat* (decreased by ~65%), *Nqo1* (decreased by ~40%), *Hmx1* (decreased by ~80%), *Gstt3* (decreased by ~40%) and *Gpx1* (decreased by ~70%) ( $p < 0.001$ ). *Gpx3* expression increased slightly. Expression of *Gstm3*, *Gstm6*, *Gpx2* did not differ between WT and  $\sigma$ 1RKO Müller cells. We measured the protein levels of SOD1, CAT and NQO1 and HMOX1, GPX1 and GPX2 in WT and  $\sigma$ 1RKO Müller cells and observed a marked decrease

in protein levels of SOD1 (decreased by ~90%), CAT (decreased by ~70%), NQO1 (decreased by ~40%) and GPX1 (decreased by ~60%) in  $\sigma$ 1RKO Müller cells compared to WT (Fig. 3B). Protein levels of HMOX-1 did not differ significantly between WT and  $\sigma$ 1RKO Müller cells (Fig. 3B). (It is unclear if this anti-HMOX1 Ab cross reacted to HMOX2, resulting in the discrepancy between HMOX1 mRNA and protein levels.) The quantification of the immunoblotting data (three independent experiments) is shown (Fig. 3C). Detection for GPX2 showed very low protein levels in both WT and  $\sigma$ 1RKO Müller cells (e.g. barely detectable by immunoblotting, data not shown).

(.) Otherwise, the discrepancy between mRNA an

### Suppression of NRF2 signaling in $\sigma$ 1RKO Müller glia

We investigated NRF2 signaling in  $\sigma$ 1RKO Müller glia versus WT because NRF2 binds the AREs found in the 5'-flanking region of *Sod1*, *Cat*, *Nqo1*, *Hmox1*, *Gstt3* and *Gpx1* [32, 44, 45]. Given the significant decrease in expression of these antioxidant genes in  $\sigma$ 1RKO Müller cells (Fig. 3), we predicted that NRF2 levels would be altered. We also investigated KEAP1, the well-recognized inhibitor of NRF2, in  $\sigma$ 1RKO versus WT Müller cells. There was a significant decrease (~60%) in *Nrf2* expression in  $\sigma$ 1RKO cells compared to WT (Fig. 4A). Concomitantly there was a marked increase in *Keap1* expression (4.38±0.56 fold change in  $\sigma$ 1RKO Müller cells versus WT) (Fig. 4A). Western blotting results showed a similar change in NRF2 (decrease) and Keap1 (increase) protein levels (Fig. 4B). Densitometry reflected ~80% decrease in NRF2 levels and ~2.5 fold increase KEAP1 in  $\sigma$ 1RKO Müller cells compared to WT (Fig. 4C). We examined NRF2 and KEAP1 using an immunocytochemical approach in Müller cells harvested from  $\sigma$ 1RKO and WT mice. We observed a marked decrease in NRF2 in  $\sigma$ 1RKO cells compared to WT (Fig. 4D) and conversely a substantial increase in KEAP1 (Fig. 4E) in  $\sigma$ 1RKO cells vs. WT. We investigated NRF2 activity using an ARE oligonucleotide-based trans-activation assay in nuclear extracts of  $\sigma$ 1RKO and WT Müller cells. There was a significant decrease (~50%) in NRF2 activity in  $\sigma$ 1RKO cells compared to WT ( $p<0.01$ ,  $p<0.001$ ) (Fig. 4F). The data suggest a role for  $\sigma$ 1R in modulating NRF2 transcriptional regulation of AREs of several antioxidant genes.

### Decreased system $x_c^-$ activity and xCT levels in $\sigma$ 1RKO Müller glia

The cystine-glutamate exchanger, system  $x_c^-$  is comprised of two proteins, xCT and 4F2hc (4F2 cell-surface antigen heavy chain, encoded by the *Slc3a2* (solute carrier family 3 member 2) gene) [46]. xCT is the unique component of the system; it has an ARE that can be activated by NRF2 [31]. We investigated the activity of the transporter and as well as xCT expression. Since system  $x_c^-$  is a freely reversible exchanger for cystine and glutamate we were able to evaluate its transport function by monitoring the  $Na^+$ -independent influx of radiolabeled glutamate as described in the methods section. We cultured WT and  $\sigma$ 1RKO Müller cells and determined that uptake of radiolabeled glutamate in WT cells was significantly greater than in  $\sigma$ 1RKO cells (252.63 ± 2.45 pmol/mg protein/15 min versus 98.86 ± 4.95 pmol/mg protein/15 min) (Fig. 5A). The kinetics of system  $x_c^-$  activity was analyzed in WT and  $\sigma$ 1RKO Müller cells. The transport function of system  $x_c^-$  was monitored by measuring the  $Na^+$ -independent uptake of radiolabeled glutamate in the

presence of increasing concentrations of un-labeled glutamate. The decreased transport activity of system  $x_c^-$  observed in  $\sigma$ 1RKO Müller cells compared with WT cells was associated with a significant decrease in the maximal velocity ( $V_{max}$ ) of the transporter but no significant difference in the substrate affinity ( $K_m$ ). The maximal velocity of glutamate uptake was ~50% less in  $\sigma$ 1RKO Müller cells (955.9 pmol/mg protein/15 min  $\pm$  52.1) compared with WT (2062.9 pmol/mg protein/15 min  $\pm$  168.8). The Michaelis constant for glutamate in  $\sigma$ 1RKO cells (65.0  $\mu$ M  $\pm$  7.2) was similar to WT cells (78.6  $\mu$ M  $\pm$  12.6).  $V_{max}$  is directly proportional to the concentration of the protein on the membrane. The unique protein component of system  $x_c^-$  is xCT, therefore we examined expression of the gene encoding xCT and the level of the protein in Müller cells from WT and  $\sigma$ 1RKO mice. The expression of xCT in  $\sigma$ 1RKO Müller cells was markedly reduced (by ~75%) compared to WT (Fig. 5C). There was a significant decrease in the level of xCT protein as well. Fig. 5D shows representative immunoblots detecting xCT in cells isolated from WT versus  $\sigma$ 1RKO mice; quantification of band densities is shown (Fig. 5E). We evaluated xCT protein levels in whole retina tissue of WT and  $\sigma$ 1R KO mice and observed a decrease in xCT levels in retinas of  $\sigma$ 1RKO mice compared to WT (Fig. 5F, 5G). The functional and molecular data suggest that activity and expression of the cystine-glutamate exchanger may be regulated by  $\sigma$ 1R.

#### Decreased GSH levels in $\sigma$ 1RKO Müller glia

The decreased activity of system  $x_c^-$ , which is important for synthesis of GSH prompted investigation of the levels of this key antioxidant in WT versus  $\sigma$ 1RKO Müller cells. We detected GSH indirectly using CMFDA, a cell-permeant chloromethyl derivative of fluorescein diacetate. Immunofluorescent imaging showed a significant decrease in cellular levels of GSH in  $\sigma$ 1RKO Müller cells from WT mice (Fig. 6A). Quantification of fluorescent intensity data are provided in Fig. 6B. We then determined intracellular GSH levels and the GSH/GSSG ratio directly using a biochemical assay and observed a dramatic depletion of GSH (WT: 401.7 $\pm$ 31.9;  $\sigma$ 1RKO: 217.7 $\pm$ 33.2,  $p$ <0.01) (Fig. 6C), and decreased GSH/GSSG ratio (8.9:1 vs 4.8:1; WT vs  $\sigma$ 1RKO,  $p$ <0.01) (Fig. 6D) were observed in  $\sigma$ 1RKO Müller cells when compared to WT. The results of these indirect and direct assessments suggest that there is a marked decrease in the levels of GSH in Müller cells lacking  $\sigma$ 1R.

#### Discussion

This study provides the first evidence that in the absence of  $\sigma$ 1R, NRF2 and KEAP1 gene and protein levels are significantly altered. The data are important because they be relevant to the remarkable neuroprotective properties observed when some ligands for the receptor are used therapeutically in models of retinopathies [10–15, 25, 27]. It is acknowledged that the data presented herein were obtained from isolated cells, which may become activated simply by being maintained under cell culture conditions. Other studies report that the level of GFAP, a marker of Müller cell activation, is very modest in cultures of Müller cells used at passage 4–5, as used in the current study [47]. Thus, useful conclusions can be made from the data that are relevant to retinal disease.

Several important findings emerge from this study. First, there was significant elevation of endogenous ROS in Müller cells isolated from  $\sigma$ 1RKO mice. Our study was initially undertaken to compare the effects of (+)-PTZ in attenuating oxidative stress in retinal Müller glial cells. We observed a decrease in ROS when WT cells were pretreated with this high affinity  $\sigma$ 1R ligand. We used Müller cells isolated from  $\sigma$ 1RKO mice in this initial experiment to test the specificity of (+)-PTZ for  $\sigma$ 1R in conferring its protective effects. As predicted, we found that (+)-PTZ treatment of  $\sigma$ 1RKO Müller cells had no effect in attenuating ROS production in H<sub>2</sub>O<sub>2</sub>-exposed cells. This confirmed earlier reports that  $\sigma$ 1R was required for (+)-PTZ to mediate anti-apoptotic effects in retinal ganglion cells [42,43]. What was not expected from these experiments, however, was that endogenous ROS would be elevated in Müller cells that were harvested from mice lacking  $\sigma$ 1R. This suggested that absence of  $\sigma$ 1R might be linked with an inherent increased level of oxidative stress in these retinal glial cells.

These intriguing findings led to a systematic evaluation of the oxidative stress response in  $\sigma$ 1RKO Müller glial cells compared to WT. We investigated the expression of genes encoding a number of well-characterized antioxidant proteins and observed significantly decreased expression of *Sod1*, *Cat*, *Nqo1*, *Hmox1*, *Gstt3*, and *Gpx1* mRNA. Several of the proteins encoded by these genes (SOD1, CAT, NQO1, GPX1) were also decreased significantly. Regarding expression of *Gpx2* and *Gpx3*, these are both members of the glutathione peroxidase (GPx) family of enzymes, which catalyze the reduction of hydrogen peroxide to water (or alcohol) typically using GSH as the reductant. In our previous microarray analysis of the  $\sigma$ 1RKO neural retina [20] we observed a significant increase in *Gpx3* in retinas of  $\sigma$ 1RKO mice (2.34 fold). GPx3 is an intracellular enzyme actively released into the plasma so the significance of its elevation in the  $\sigma$ 1RKO neural retina is not clear, nor its elevation in the present study of Müller cells. Most studies of glutathione peroxidase in retina have focused on GPx1 [48,49], therefore in our studies we investigated its expression in  $\sigma$ 1RKO Müller cells and found a significant decrease at the gene and protein level. In our investigation of *Gpx2* gene expression; we observed no significant difference between  $\sigma$ 1RKO Müller cells versus WT. Indeed, the level of the GPX2 protein was minimally detected in the Müller cells. *GPx2* is mainly expressed in the epithelium lining the gastrointestinal tract [50], thus its expression in retinal Müller cells may be quite low. Also observed in the earlier microarray screening of  $\sigma$ 1RKO neural retina [20] was a slight increase in expression of two glutathione-s-transferase genes *Gstm6* (1.47 fold, p=0.049) and *Gstm3* (1.45 fold, p=0.055). In the current study using Müller cells we investigated the expression of these genes and found no change in gene expression. This suggests that within retinas of  $\sigma$ 1RKO mice, there are cells that are changing expression of genes encoding the two GSTs, but they are not likely Müller cells.

Each of these antioxidant genes harbors an antioxidant response element, which is located in the 5' flanking region of many phase II detoxifying and antioxidant genes [47]. ARE activation triggers the transcription of genes involved in antioxidant defense including those observed in this study (*Sod1*, *Cat*, *Nqo1*, *Hmox1*, *Gstt3*, *Gpx1*) by a mechanism that involves the NRF2-KEAP1 pathway [44, 51,52]. We examined the levels of these two proteins in Müller cells isolated from WT and  $\sigma$ 1RKO mice. NRF2 is a ubiquitously expressed member

of the Cap'n'Collar family of bZIP proteins [53]. Under basal conditions, NRF2-dependent transcription is repressed by KEAP1. Under oxidative stress conditions, NRF2 protein escapes KEAP1-mediated repression, translocates to the nucleus and induces ARE-dependent gene expression [51]. We observed a significant decrease in NRF2 gene and protein expression in the  $\sigma$ 1RKO Müller cells compared with WT, while at the same time observed an increase in KEAP1 gene and protein expression in these cells. We also observed a significant decrease in NRF2-ARE binding activity in  $\sigma$ 1RKO Müller cells compared with WT. We speculate that the altered antioxidant gene levels observed in  $\sigma$ 1RKO Müller cells reflect perturbation of the NRF2-KEAP1 pathway. In related experiments, it has been demonstrated that when COS-7 cells are transfected with *Sigma1r*, there is a concomitant upregulation of *Nqo1* and *Sod1* via the activation of ARE [26]. Taken collectively, it appears that  $\sigma$ 1R modulates oxidative stress genes via its action on NRF2-KEAP1.

Another protein that is actively involved in the antioxidant cellular response and whose transcription is regulated by NRF2 binding to ARE is xCT [31]. xCT is a 502 amino acid protein also named SLC7A11. It is the specific light chain subunit of the cystine-glutamate exchanger known as system  $x_c^-$ . System  $x_c^-$  is a sodium-independent, chloride-dependent antiporter of cystine and glutamate. It is comprised of xCT as one unit and the promiscuous 4F2 heavy chain (4F2hc/CD98/SCL3A2) as the other unit [30]. System  $x_c^-$  is particularly important for the synthesis of GSH, which is present in millimolar quantities in cells and is one of the most important small molecule cellular antioxidants. GSH is a tripeptide consisting of the amino acids glutamate, glycine and cysteine. The rate-limiting amino acid for GSH synthesis is cysteine, which can be imported into cells directly or in its oxidized form (cystine) via system  $x_c^-$ . System  $x_c^-$  is known to be present in retinal Müller glial cells [54,55]. We studied the function of system  $x_c^-$  in Müller cells harvested from  $\sigma$ 1RKO and WT mice and also examined the expression of xCT at the gene and protein level. We observed a marked reduction in the activity of system  $x_c^-$  in  $\sigma$ 1RKO cells compared to WT. Our kinetic analysis suggested a decrease in  $V_{max}$ , which was accompanied by a decrease, not only in the expression of the gene encoding xCT, but also in the level of the protein as well. The decreased GSH levels that we observed in the  $\sigma$ 1RKO Müller glia may reflect the diminished activity of this key cystine uptake system. The current data regarding decreased xCT gene and protein levels using Müller cells are consistent with our earlier microarray analysis showing significantly decreased expression of *Slc7a11* ( $-1.94$ ,  $p=0.01$ ) in  $\sigma$ 1RKO neural retina compared to WT [20]. In the present study, we confirmed the decreased xCT gene and protein levels in neural retina also of  $\sigma$ 1RKO mice compared to WT.

The compromised mechanisms for managing oxidative stress detected in retinal Müller glial cells may play a role in the late onset retinal degeneration that is observed in the  $\sigma$ 1RKO mouse [35]. Though no overt retinal pathology is observed during the early post-natal period, ultrastructural evidence of axonal disruption is evident in the optic nerve head of  $\sigma$ 1RKO mice as early as 6 months of age. By 12 months significantly decreased ERG b-wave amplitudes and diminished negative scotopic threshold responses, consistent with inner retinal dysfunction, are detected in  $\sigma$ 1RKO mice. These mutant mice also demonstrate increased susceptibility to stress as seen by more rapid retinal degeneration in mice with diabetes [42] or to optic nerve crush [56].

$\sigma$ 1R is an enigmatic protein. Although its expression levels differ between tissues, it appears to be expressed in all cell types examined to date and in several organelles (plasma membrane, nucleus, mitochondria and the endoplasmic reticulum). Indeed, its localization to the ER and mitochondrial associated membrane has resulted in many investigations of  $\sigma$ 1R as a mediator of ER stress [16, 57].  $\sigma$ 1R has no other known family members, since “ $\sigma$ 2R”, which shares some ligand binding properties with  $\sigma$ 1R, is suggested to be the binding site in the progesterone receptor membrane component 1 (PGRMC1) protein complex [58].

The current findings provide compelling evidence that levels of Nrf2 and Keap1 are altered in the absence of  $\sigma$ 1R, which sets the stage for future studies of  $\sigma$ 1R as a major regulator of the Nrf2-Keap1 pathway. Although the current data were obtained in retinal glial cells, they are relevant to other organs/tissues as well. Indeed, in many diseases in which oxidative stress is implicated, there may be a major role of  $\sigma$ 1R as a mediator of the key antioxidant pathway Nrf2-Keap1. These present findings in conjunction with the reports that  $\sigma$ 1R acts a modulator of oxidative stress and activates ARE [26] support this putative role.

## Acknowledgments

Acknowledgement of research support: NIH grant R01 EY014560 and the James and Jean Culver Vision Discovery Institute.

## Literature cited

1. Frey T, Antonetti DA. Alterations to the blood-retinal barrier in diabetes: cytokines and reactive oxygen species. *Antioxid Redox Signal*. 2011; 15:1271–1284. [PubMed: 21294655]
2. Cuenca N, Fernández-Sánchez L, Campello L, Maneu V, De la Villa P, Lax P, Pinilla I. Cellular responses following retinal injuries and therapeutic approaches for neurodegenerative diseases. *Prog Retin Eye Res*. 2014 In Press.
3. Tsai SY, Hayashi T, Harvey BK, Wang Y, Wu WW, Shen RF, Zhang Y, Becker KG, Hoffer BJ, Su TP. Sigma-1 receptors regulate hippocampal dendritic spine formation via a free radical-sensitive mechanism involving Rac1xGTP pathway. *Proc Natl Acad Sci*. 2009; 106:22468–73. [PubMed: 20018732]
4. Brune S, Priel S, Wünsch B. Structure of the  $\sigma$ 1 receptor and its ligand binding site. *J Med Chem*. 2013; 56:9809–9819. [PubMed: 23964901]
5. Hanner M, Moebius FF, Flandorfer A, Knaus HG, Striessnig J, Kempner E, Glossmann H. Purification, molecular cloning, and expression of the mammalian sigma1-binding site. *Proc Natl Acad Sci*. 1996; 93:8072–8077. [PubMed: 8755605]
6. Kekuda R, Prasad PD, Fei YJ, Leibach FH, Ganapathy V. Cloning and functional expression of the human type 1 sigma receptor (hSigmaR1). *Biochem Biophys Res Commun*. 1996; 229:553–558. [PubMed: 8954936]
7. Seth P, Leibach FH, Ganapathy V. Cloning and structural analysis of the cDNA and the gene encoding the murine type 1 sigma receptor. *Biochem Biophys Res Commun*. 1997; 241:535–540. [PubMed: 9425306]
8. Fontanilla D, Johannessen M, Hajipour AR, Cozzi NV, Jackson MB, Ruoho AE. The hallucinogen N,N-dimethyltryptamine (DMT) is an endogenous sigma-1 receptor regulator. *Science*. 2009; 323:934–937. [PubMed: 19213917]
9. Griesmaier E, Posod A, Gross M, Neubauer V, Wegleiter K, Hermann M, Urbanek M, Keller M, Kiechl-Kohlendorfer U. Neuroprotective effects of the sigma-1 receptor ligand PRE-084 against excitotoxic perinatal brain injury in newborn mice. *Exp Neurol*. 2012; 237:388–395. [PubMed: 22771763]



10. Zhang Y, Shi Y, Qiao L, Sun Y, Ding W, Zhang H, Li N, Chen D. Sigma-1 receptor agonists provide neuroprotection against gp120 via a change in bcl-2 expression in mouse neuronal cultures. *Brain Res.* 2012; 1431:13–22. [PubMed: 22133307]
11. Yang S, Bhardwaj A, Cheng J, Alkayed NJ, Hurn PD, Kirsch JR. Sigma receptor agonists provide neuroprotection in vitro by preserving bcl-2. *Anesth Analg.* 2007; 104:1179–84. [PubMed: 17456670]
12. Tchandre KT, Yorio T. Sigma-1 receptors protect RGC-5 cells from apoptosis by regulating intracellular calcium, Bax levels, and caspase-3 activation. *Invest Ophthalmol Vis Sci.* 2008; 49:2577–2588. [PubMed: 18296662]
13. Dun Y, Thangaraju M, Prasad P, Ganapathy V, Smith SB. Prevention of excitotoxicity in primary retinal ganglion cells by (+)-pentazocine, a sigma receptor-1 specific ligand. *Invest Ophthalmol Vis Sci.* 2007; 48:4785–4794. [PubMed: 17898305]
14. Cantarella G, Bucolo C, Di Benedetto G, Pezzino S, Lempereur L, Calvagna R, Clementi S, Pavone P, Fiore L, Bernardini R. Protective effects of the sigma agonist Pre-084 in the rat retina. *Br J Ophthalmol.* 2007; 91:382–4.
15. Smith SB, Duplantier J, Dun Y, Mysona B, Roon P, Martin PM, Ganapathy V. In vivo protection against retinal neurodegeneration by sigma receptor 1 ligand (+)-pentazocine. *Invest Ophthalmol Vis Sci.* 2008; 49:4154–4161. [PubMed: 18469181]
16. Hayashi T, Su TP. Sigma-1 receptor chaperones at the ER-mitochondrion interface regulate Ca(2+) signaling and cell survival. *Cell.* 2007; 131:596–610. [PubMed: 17981125]
17. Malhotra JD, Kaufman RJ. Endoplasmic reticulum stress and oxidative stress: a vicious cycle or a double-edged sword? *Antioxid Redox Signal.* 2007; 9:2277–2293. [PubMed: 17979528]
18. Wang L, Eldred JA, Sidaway P, Sanderson J, Smith AJ, Bowater RP, Reddan JR, Wormstone IM. Sigma 1 receptor stimulation protects against oxidative damage through suppression of the ER stress responses in the human lens. *Mech Ageing Dev.* 2012; 133:665–74. [PubMed: 23041531]
19. Omi T, Tanimukai H, Kanayama D, Sakagami Y, Tagami S, Okochi M, Morihara T, Sato M, Yanagida K, Kitasyoji A, Hara H, Imaizumi K, Maurice T, Chevallier N, Marchal S, Takeda M, Kudo T. Fluvoxamine alleviates ER stress via induction of Sigma-1 receptor. *Cell Death Dis.* 2014; 5:e1332. [PubMed: 25032855]
20. Ha Y, Shanmugam AK, Markand S, Zorrilla E, Ganapathy V, Smith SB. Sigma receptor 1 modulates ER stress and Bcl2 in murine retina. *Cell Tissue Res.* 2014; 356:15–27. [PubMed: 24469320]
21. Mori T, Hayashi T, Hayashi E, Su TP. Sigma-1 receptor chaperone at the ER-mitochondrion interface mediates the mitochondrion-ER-nucleus signaling for cellular survival. *PLoS One.* 2013; 8:e76941. [PubMed: 24204710]
22. Ortega-Roldan JL, Ossa F, Schnell JR. Characterization of the human sigma-1 receptor chaperone domain structure and binding immunoglobulin protein (BiP) interactions. *J Biol Chem.* 2013; 288:21448–41457. [PubMed: 23760505]
23. Hayashi T, Hayashi E, Fujimoto M, Sprong H, Su TP. The lifetime of UDP-galactose:ceramide galactosyltransferase is controlled by a distinct endoplasmic reticulum-associated degradation (ERAD) regulated by sigma-1 receptor chaperones. *J Biol Chem.* 2012; 287:43156–43169. [PubMed: 23105111]
24. Mitsuda T, Omi T, Tanimukai H, Sakagami Y, Tagami S, Okochi M, Kudo T, Takeda M. Sigma-1Rs are upregulated via PERK/eIF2 $\alpha$ /ATF4 pathway and execute protective function in ER stress. *Biochem Biophys Res Commun.* 2011; 415:519–525. [PubMed: 22079628]
25. Ha Y, Dun Y, Thangaraju M, Duplantier J, Dong Z, Liu K, Ganapathy V, Smith SB. Sigma receptor 1 modulates endoplasmic reticulum stress in retinal neurons. *Invest Ophthalmol Vis Sci.* 2011; 52:527–540. [PubMed: 20811050]
26. Pal A, Fontanilla D, Gopalakrishnan A, Chae YK, Markley JL, Ruoho AE. The sigma-1 receptor protects against cellular oxidative stress and activates antioxidant response elements. *Eur J Pharmacol.* 2012; 682:12–20. [PubMed: 22381068]
27. Bucolo C, Drago F, Lin LR, Reddy VN. Sigma receptor ligands protect human retinal cells against oxidative stress. *Neuroreport.* 2006; 17:287–291. [PubMed: 16462599]

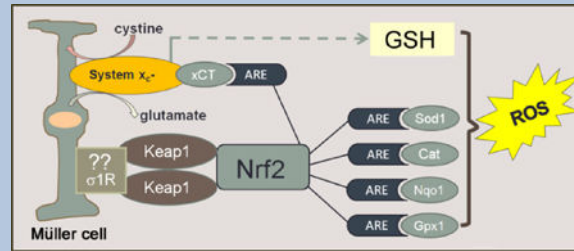
28. Jiang G, Mysona B, Dun Y, Gnana-Prakasam JP, Pabla N, Li W, Dong Z, Ganapathy V, Smith SB. Expression, subcellular localization, and regulation of sigma receptor in retinal Müller cells. *Invest Ophthalmol Vis Sci*. 2006; 47:5576–5582. [PubMed: 17122151]
29. Reichenbach A, Bringmann A. New functions of Müller cells. *Glia*. 2013; 61:651–678. [PubMed: 23440929]
30. Bannai S, Kitamura E. Transport interaction of L-cystine and L-glutamate in human diploid fibroblasts in culture. *J Biol Chem*. 1980; 255:2372–2376. [PubMed: 7358676]
31. Lewerenz J, Hewett SJ, Huang Y, Lambros M, Gout PW, Kalivas PW, Massie A, Smolders I, Methner A, Pergande M, Smith SB, Ganapathy V, Maher P. The cystine/glutamate antiporter system x(c)(-) in health and disease: from molecular mechanisms to novel therapeutic opportunities. *Antioxid Redox Signal*. 2013; 18:522–555. [PubMed: 22667998]
32. Gupta RK, Patel AK, Shah N, Chaudhary AK, Jha UK, Yadav UC, Gupta PK, Pakuwal U. Oxidative stress and antioxidants in disease and cancer: a review. *Asian Pac J Cancer Prev*. 2014; 15:4405–4409. [PubMed: 24969860]
33. Sporn MB, Liby KT. NRF2 and cancer: the good, the bad and the importance of context. *Nat Rev Cancer*. 2012; 12:564–571. [PubMed: 22810811]
34. Sabino V, Cottone P, Parylak SL, Steardo L, Zorrilla EP. Sigma-1 receptor knockout mice display a depressive-like phenotype. *Behav Brain Res*. 2009; 198:472–476. [PubMed: 19100292]
35. Ha Y, Saul A, Tawfik A, Williams C, Bollinger K, Smith R, Tachikawa M, Zorrilla E, Ganapathy V, Smith SB. Late-onset inner retinal dysfunction in mice lacking sigma receptor 1 ( $\sigma R1$ ). *Invest Ophthalmol Vis Sci*. 2011; 52:7749–7760. [PubMed: 21862648]
36. Shanmugam A, Wang J, Markand S, Perry RL, Tawfik A, Zorrilla E, Ganapathy V, Smith SB. Sigma Receptor 1 activation attenuates release of inflammatory cytokines MIP1, MIP2, MIP3 $\alpha$  and IL12 (p40/p70) by retinal Müller glial cells. *J Neurochem*. 2015 In Press.
37. Hicks D, Courtois Y. The growth and behaviour of rat retinal Müller cells in vitro. 1. An improved method for isolation and culture. *Exp Eye Res*. 1990; 51:119–129. [PubMed: 2387332]
38. Ola MS, Moore PM, Maddox D, El-Sherbeny A, Huang W, Roon P, Agarwal N, Ganapathy V, Smith SB. Analysis of Sigma Receptor ( $\sigma R1$ ) expression in retinal ganglion cells cultured under hyperglycemic conditions and in diabetic mice. *Brain Res Mol Brain Res*. 2002; 107:97–107. [PubMed: 12425939]
39. Tetz LM, Kamau PW, Cheng AA, Meeker JD, Loch-Carusio R. Troubleshooting the dichlorofluorescein assay to avoid artifacts in measurement of toxicant-stimulated cellular production of reactive oxidant species. *J Pharmacol Toxicol Methods*. 2013; 67:56–60. [PubMed: 23380227]
40. Sarthy VP, Pignataro L, Pannicke T, Weick M, Reichenbach A, Harada T, Tanaka K, Marc R. Glutamate transport by retinal Muller cells in glutamate/aspartate transporter-knockout mice. *Glia*. 2005; 49:184–196. [PubMed: 15390100]
41. Bridges CC, Kekuda R, Wang H, Prasad PD, Mehta P, Huang W, Smith SB, Ganapathy V. Structure, function, and regulation of human cystine/glutamate transporter in retinal pigment epithelial cells. *Invest Ophthalmol Vis Sci*. 2001; 42:47–54. [PubMed: 11133847]
42. Ha Y, Saul A, Tawfik A, Zorrilla EP, Ganapathy V, Smith SB. Diabetes accelerates retinal ganglion cell dysfunction in mice lacking sigma receptor 1. *Mol Vis*. 2012; 18:2860–2870. [PubMed: 23233788]
43. Mueller BH, Park Y, Daudt DR, Ma HY, Akopova I, Stankowska DL, Clark AF, Yorio T. Sigma-1 receptor stimulation attenuates calcium influx through activated L-type Voltage Gated Calcium Channels in purified retinal ganglion cells. *Exp Eye Res*. 2013; 107:21–31. [PubMed: 23183135]
44. Muthusamy VR, Kannan S, Sadhaasivam K, Gounder SS, Davidson CJ, Boeheme C, Hoidal JR, Wang L, Rajasekaran NS. Acute exercise stress activates Nrf2/ARE signaling and promotes antioxidant mechanisms in the myocardium. *Free Rad Biol Med*. 2012; 52:366–376. [PubMed: 22051043]
45. Banning A, Deubel S, Kluth D, Zhou Z, Brigelius-Flohe R. The GI-GPx gene is a target for Nrf2. *Mol Cell Bio*. 2005; 25:4914–4923. [PubMed: 15923610]
46. Bridges RJ, Natale NR, Patel SA. System Xc- cystine/glutamate antiporter: an update on molecular pharmacology and roles within the CNS. *British J Pharmacology*. 2012; 165:20–34.

47. Umapathy NS, Li W, Mysona BA, Smith SB, Ganapathy V. Expression and function of glutamine transporters SN1 (SNAT3) and SN2 (SNAT5) in retinal Müller cells. *Invest Ophthalmol Vis Sci.* 2005; 46:3980–3987. [PubMed: 16249471]
48. Tan SM, Stefanovic N, Tan G, Wilkinson-Berka JL, de Haan JB. Lack of the antioxidant glutathione peroxidase-1 (GPx1) exacerbates retinopathy of prematurity in mice. *Invest Ophthalmol Vis Sci.* 2013; 54:555–62. [PubMed: 23287791]
49. Gosbell AD, Stefanovic N, Scurr LL, Pete J, Kola I, Favilla I, de Haan JB. Retinal light damage: structural and functional effects of the antioxidant glutathione peroxidase-1. *Invest Ophthalmol Vis Sci.* 2006; 47:2613–22. [PubMed: 16723478]
50. Florian S, Wingler K, Schmehl K, Jacobasch G, Kreuzer OJ, Meyerhof W, Brigelius-Flohé R. Cellular and subcellular localization of gastrointestinal glutathione peroxidase in normal and malignant human intestinal tissue. *Free Radic Res.* 2001 Dec; 35(6):655–63. [PubMed: 11811519]
51. Rushmore TH, Morton MR, Pickett CB. The antioxidant responsive element: Activation by oxidative stress and identification of the DNA consensus sequence required for functional activity. *J Biol Chem.* 1991; 266:1632–1163.
52. Gan L, Johnson JA. Oxidative damage and the Nrf2-ARE pathway in neurodegenerative diseases. *Biochim Biophys Acta.* 2014; 1842:1208–1218. [PubMed: 24382478]
53. Zhang DD. Mechanistic studies of the Nrf2-Keap1 signaling pathway. *Drug Metab Rev.* 2006; 38:769–789. [PubMed: 17145701]
54. Tomi M, Funaki T, Abukawa H, Katayama K, Kondo T, Ohtsuki S, Ueda M, Obinata M, Terasaki T, Hosoya K. Expression and regulation of L-cystine transporter, system xc<sup>-</sup>, in the newly developed rat retinal Müller cell line (TR-MUL). *Glia.* 2003; 43:208–17. [PubMed: 12898700]
55. Mysona B, Dun Y, Duplantier J, Ganapathy V, Smith SB. Effects of hyperglycemia and oxidative stress on the glutamate transporters GLAST and system xc<sup>-</sup> in mouse retinal Müller glial cells. *Cell Tissue Res.* 2009; 335:477–488. [PubMed: 19156441]
56. Mavlyutov TA, Nickells RW, Guo LW. Accelerated retinal ganglion cell death in mice deficient in the Sigma-1 receptor. *Mol Vis.* 2011; 26:1034–1043. [PubMed: 21541278]
57. Mori T, Hayashi T, Hayashi E, Su TP. Sigma-1 receptor chaperone at the ER-mitochondrion interface mediates the mitochondrion-ER-nucleus signaling for cellular survival. *PLoS One.* 2013; 8(10)
58. Xu J, Zeng C, Chu W, Pan F, Rothfuss JM, Zhang F, Tu Z, Zhou D, Zeng D, Vangveravong S, Johnston F, Spitzer D, Chang KC, Hotchkiss RS, Hawkins WG, Wheeler KT, Mach RH. Identification of the PGRMC1 protein complex as the putative sigma-2 receptor binding site. *Nat Commun.* 2011; 2:380. [PubMed: 21730960]

### Highlights

- Oxidative stress is a major contributor to retinal disease.
- The role of  $\sigma$ 1R in mediating oxidative stress was explored in  $\sigma$ 1RKO mouse retinal Müller cells (MC).
- $\sigma$ 1RKO MCs manifest elevated ROS, perturbed antioxidant balance and suppression of Nrf2 signaling.
- Function and expression of system  $x_c^-$ , the cystine-glutamate exchanger is impaired in  $\sigma$ 1RKO MCs.
- Oxidative stress-mediating function of retinal MCs may be compromised in the absence of  $\sigma$ 1R.

## Schematic of paper



Oxidative stress in the form of reactive oxygen species (ROS) figures prominently in retinal diseases. The Müller glial cell is a major mediator of retinal homeostasis. In this paper, Müller cells harvested from mice lacking  $\sigma 1R$ , a putative molecular chaperone, showed an increase endogenous production of ROS. This was accompanied by decreased expression of a number of antioxidant proteins, which are known to harbor antioxidant response elements (ARE). Nrf2, which is a major regulator of oxidative stress through its activation of AREs was decreased at the gene, protein and activity level; its major regulatory protein Keap1 was increased. The expression and activity of the cystine-glutamate exchanger was also decreased in Müller cells lacking  $\sigma 1R$ . Taken collectively, the data support a key role for  $\sigma 1R$  in modulation of oxidative stress in retina.

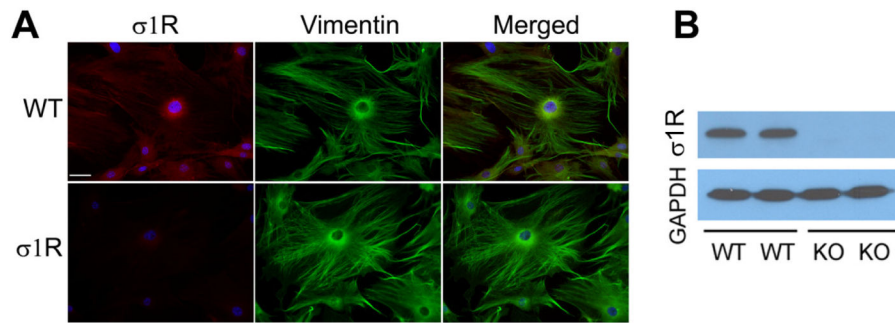


**Fig. 1. Analysis of  $\sigma$ 1R expression in mouse Müller cells**

(A) Müller cells harvested from WT (wildtype) and  $\sigma$ 1RKO (knockout) mice were cultured as described and subjected to immunocytochemistry to confirm the glial origin of the cells using vimentin (green fluorescence) or to detect  $\sigma$ 1R (red fluorescence); DAPI was used to label nuclei blue. Calibration bar = 100  $\mu$ m. (B) Immunoblotting analysis to detect  $\sigma$ 1R in WT and  $\sigma$ 1RKO Müller cells, the single band detected in WT samples has the expected size  $M_r$  25–27 kD. Membranes were reprobbed with antibody against GAPDH as a loading control.



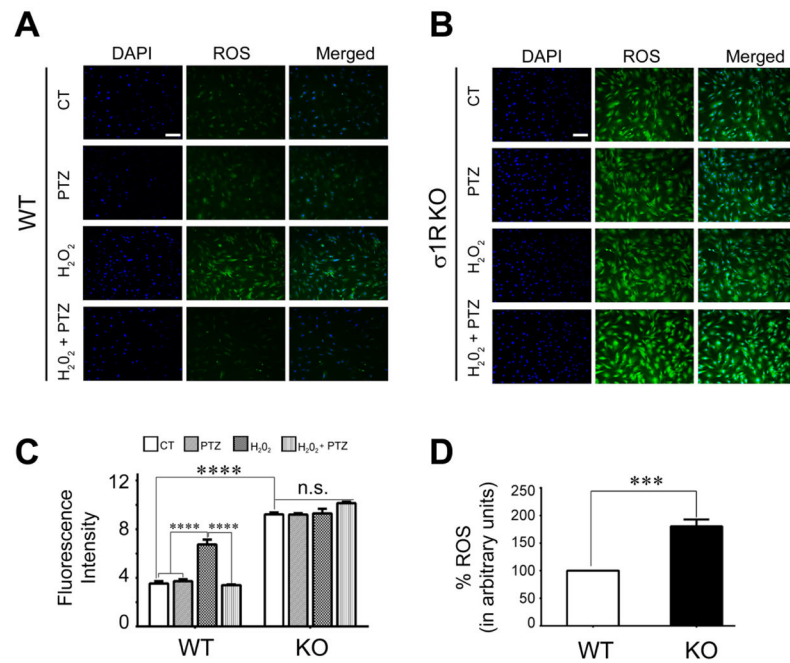


**Fig. 2. Analysis of ROS levels in WT and  $\sigma$ 1RKO mouse Müller cells**

Fluorescent detection of reactive oxygen species (ROS) using CellROX® Green Reagent. Müller cells from WT (wildtype, A) or  $\sigma$ 1RKO (knockout, B) mice were seeded on coverslips for 18 h. Cells either were or were not (control) exposed for 6 h to 200 $\mu$ M H<sub>2</sub>O<sub>2</sub> in the presence or absence of (+)-PTZ, including cells treated with (+)-PTZ alone, they were incubated with CellROX® Green Reagent to detect ROS as described. Green fluorescent signals of ROS in WT and  $\sigma$ 1RKO cells were visualized by epifluorescence; DAPI was used to label nuclei (blue). Scale bar, 100  $\mu$ m. (C) Quantification of fluorescent intensity reflecting ROS levels of data shown in panels (A) and (B) in Müller cells. (D) ROS levels were quantified in WT and  $\sigma$ 1RKO Müller cells using an assay to detect the oxidative conversion of carboxyl-DCFH-DA to the highly fluorescent carboxyl-DCF (495nm excitation/527nm emission). Data are mean  $\pm$  S.E.M of triplicate measurements \*\*\*  $p < 0.001$ ; \*\*\*\*  $p < 0.0001$ . (CT = control, PTZ = (+)-pentazocine treated).

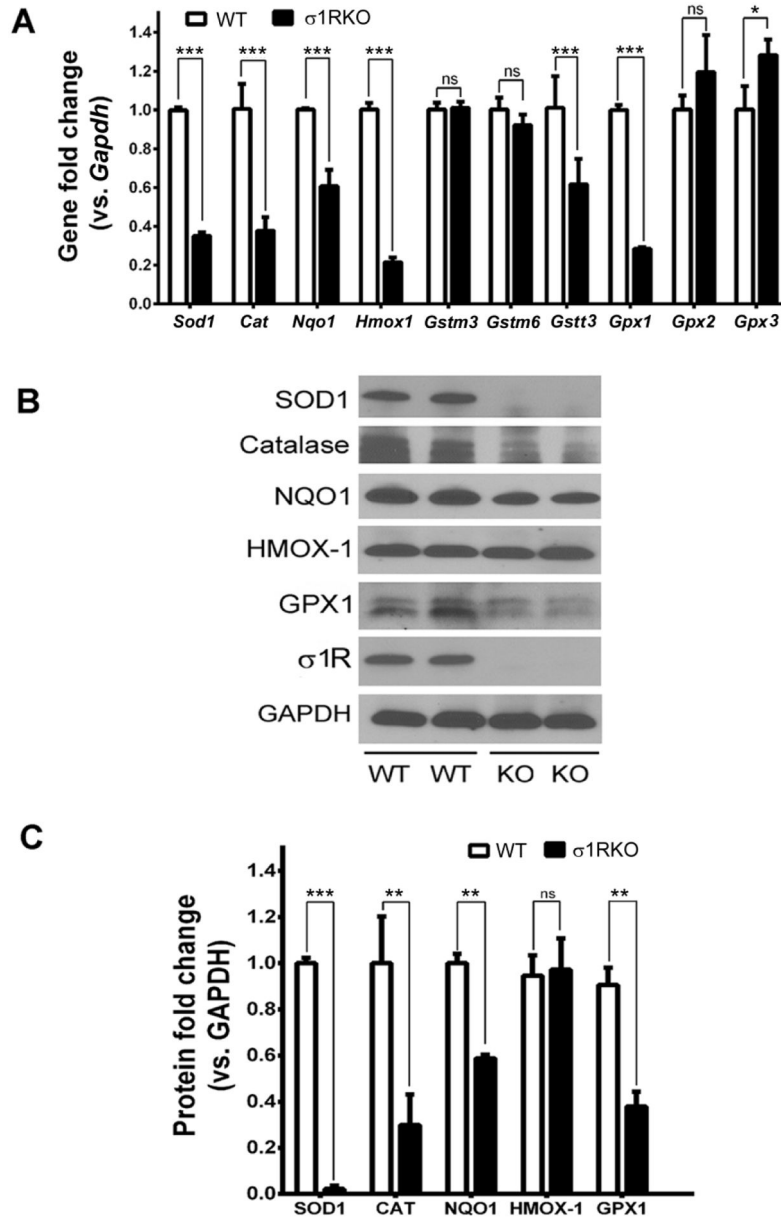


**Fig. 3. Analysis of antioxidant genes and proteins in WT and  $\sigma$ 1RKO Müller cells**  
 (A) Quantitative real-time RT-PCR analysis of *Sod1*, *Cat*, *Nqo1*, *Hmox1*, *Gstm3*, *Gstm6*, *Gstt3*, *Gpx1*, *Gpx2*, *Gpx3* mRNAs in WT (wildtype) and  $\sigma$ 1RKO (knockout) mouse Müller cells. Error bars represent mean  $\pm$  S.E.M from four separate experiments (n=4). Representative immunoblots detecting levels of SOD1, CAT, NQO1, HMOX1, GPX1 and  $\sigma$ 1R in WT and  $\sigma$ 1RKO Müller cells (B) and quantification of band densities (C). Error bars represent mean  $\pm$  S.E.M from three separate experiments (n=3). \* $p$ <0.05, \*\*  $p$ < 0.01, \*\*\* $p$ < 0.001.

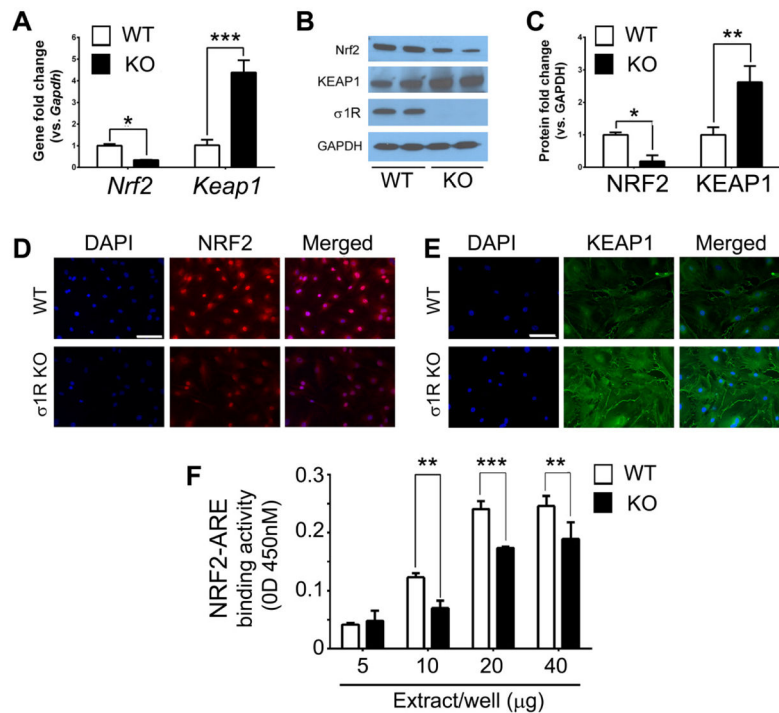


**Fig. 4. Analysis of *Nrf2* and *Keap1* (gene and protein) in WT and  $\sigma$ 1RKO Müller cells**  
 (A) Quantitative real-time RT-PCR analysis of *Nrf2* and *Keap1* mRNA extracted from WT (wildtype) and  $\sigma$ 1RKO (knockout) mouse Müller cells. The data are mean  $\pm$  S.E.M from four separate experiments (n=4). (B) Representative immunoblotting to detect NRF2 and KEAP1 following protein extraction from WT and  $\sigma$ 1RKO Müller cells. (C) Quantification of immunoblotting data. Error bars represent mean  $\pm$  S.E.M from three separate experiments (n=3). Immunocytochemistry to detect NRF2 (D) and KEAP1 (E) in WT and  $\sigma$ 1RKO Müller cells. Scale bar = 100  $\mu$ m. (F) NRF2/ARE binding activity, assayed as described in the text; the data represent values obtained at 450 nm (mean  $\pm$  SEM) for three separate experiments. (\*  $p < 0.05$ , \*\* $p < 0.01$ , \*\*\* $p < 0.001$ ).

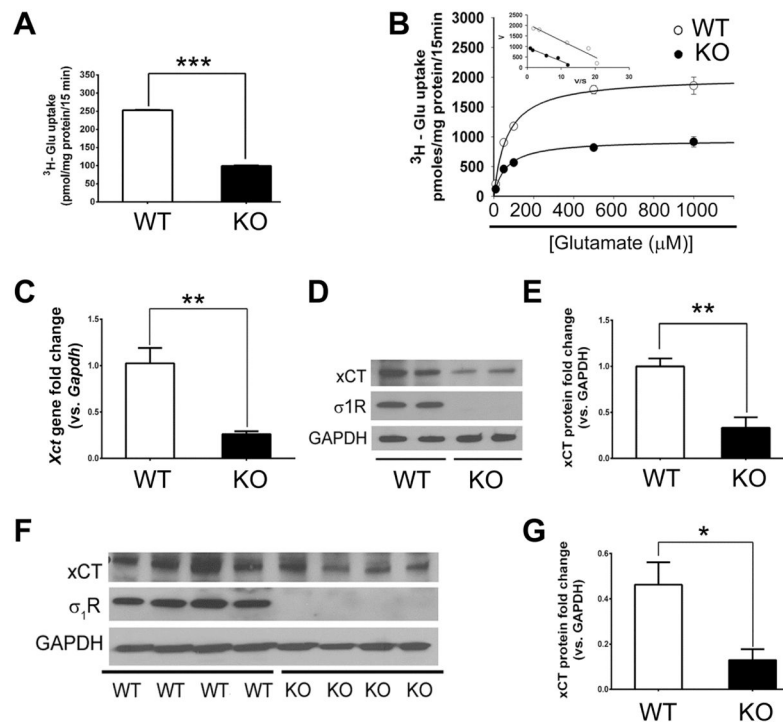


**Fig. 5. Inhibition of xCT uptake and expression level in  $\sigma$ 1RKO Müller cells and neural retina** (A) WT (wildtype) and  $\sigma$ 1RKO (knockout) mouse Müller cells were cultured as described and uptake of [ $^3$ H] glutamate by xCT was assessed as described. (B) Kinetic analysis of system  $x_c^-$  in WT and  $\sigma$ 1RKO Müller cells; the uptake of [ $^3$ H]-glutamate by the  $\text{Na}^+$ -independent system  $x_c^-$  was assessed using increasing amounts of non-radioactive glutamate ranging from 10.0  $\mu\text{M}$  to 1000  $\mu\text{M}$ . The rate of glutamate uptake (pmole/mg/15 min) is shown as a function of glutamate concentration ( $\mu\text{M}$ ). The inset is an Eadie-Hofstee plot of  $V$ , uptake velocity (pmole/mg/15 min) versus  $V/S$  where  $S$  is non-radioactive glutamate concentration ( $\mu\text{M}$ ). Values presented are means  $\pm$  SE from 3 independent experiments performed in duplicate. (C) qRT-PCR analysis of *Xct* mRNA isolated from WT and  $\sigma$ 1RKO Müller cells. Error bars represents mean  $\pm$  S.E.M from three separate experiments. Immunoblotting (D) and quantification (E) indicated a significant decrease in xCT in  $\sigma$ 1RKO Müller cells. Error bars represents mean  $\pm$  S.E.M from four separate experiments ( $n=4$ ). Immunoblotting (F) and quantification (G) demonstrated a marked decrease of xCT in whole retinal tissue isolated from  $\sigma$ 1RKO mice compared with WT. Error bars represents mean  $\pm$  S.E.M from four separate experiments ( $n=4$ ). \*  $p < 0.05$ ; \*\*  $p < 0.01$ , \*\*\*  $p < 0.001$ .

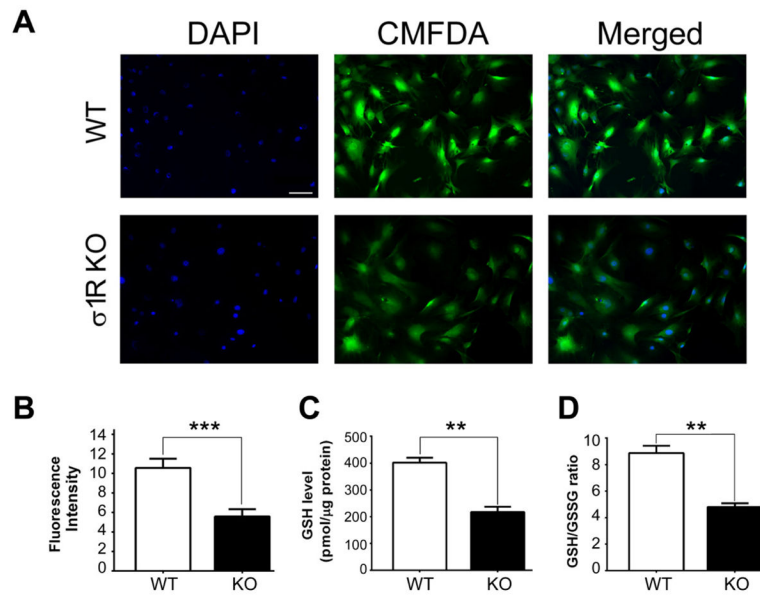


**Fig. 6. Detection of GSH levels in WT and  $\sigma$ 1RKO Müller cells**

(A) WT (wildtype) and  $\sigma$ 1RKO (knockout) mouse Müller cells were cultured as described, cellular GSH levels were assessed using fluorescence detection of CMFDA (1  $\mu$ M). Scale bar = 100  $\mu$ m. (B) Quantification of fluorescent intensity. ( $p < 0.001$ ). Cellular GSH levels and GSH/GSSG were determined as described in the text. (C) GSH levels (pmol/ $\mu$ g protein) detection in WT and  $\sigma$ 1RKO Müller cells ( $p < 0.01$ ). (D) Glutathione redox ratio (GSH/GSSG) determined in WT and  $\sigma$ 1RKO Müller cells ( $p < 0.01$ ). Each experiment was performed in triplicate.

**Table 1**

Sequences of primers used for real-time quantitative reverse transcription plus the polymerase chain reaction

Gene	NCBI Accession Number	Primer Sequence	Product size (bp)
<i>Sod1</i>	NM_011434	Forward	5'-AACCCAGTTGTGTGTCAGGAC-3'
		Reverse	5'-CCACCATGTTCTTAGAGTGAGG-3'
<i>Catalase</i>	NM_009804	Forward	5'-AGCGACCATGAAAGCAGTG-3'
		Reverse	5'-TCCGGCTCTCTGCAAAAGTGTG-3'
<i>Nqo1</i>	NM_008706	Forward	5'-AGGATGGGAGGTACTCGAATC-3'
		Reverse	5'-AGGGCTCCTTCCCTTATATGCTA-3'
<i>Hmox1</i>	NM_010442	Forward	5'-AAGCCGAGAAATGCTGAGTTC-3'
		Reverse	5'-GCCGTAGATATGGTACAAGGA-3'
<i>Gsim3</i>	NM_010359	Forward	5'-CCCCAACTTTTACCTAAAGC-3'
		Reverse	5'-GGTGTCATAACTTGGTTCCTCA-3'
<i>Gsim6</i>	NM_008184	Forward	5'-ACAGTTCATGTACACTCGAAT-3'
		Reverse	5'-TGGCTTCCGTTTCTCAAAAGTC-3'
<i>Gstf3</i>	NM_133994	Forward	5'-GGATGGGACTTCGTCITGG-3'
		Reverse	5'-TCAGGAGGTACGGGCTGTC-3'
<i>Nrf2</i>	NM_010902	Forward	5'-TAGATGACCATGAGTCGGTTGC-3'
		Reverse	5'-GCCAAAACCTTGCTCCATGTCC-3'
<i>Keap1</i>	NM_016679	Forward	5'-TGCCCTGTGGTCAAAAGTG-3'
		Reverse	5'-GGTTCGGTTACCGTCTCTGC-3'
<i>αCT</i>	NM_011990	Forward	5'-GGCACCGTCATCGGATCAG-3'
		Reverse	5'-CTCCACAGGCAGACCAGAAAA-3'
<i>Gpx1</i>	NM_008160	Forward	5'-AGTCCACCCTGTATGCCCTTCT-3'
		Reverse	5'-GAGACGGGACATTCATCAATGA-3'
<i>Gpx2</i>	NM_030677	Forward	5'-GCCTCAAAGTATGTCGGACCCTG-3'
		Reverse	5'-GGAGAACGGGTCAATCAAGGG-3'
<i>Gpx3</i>	NM_008161	Forward	5'-CCTTTTAAATCAGTATGCAGGCA-3'
		Reverse	5'-CAAGCCAAATGGCCCAAGTT-3'
<i>GAPDH</i>	NM_008084	Forward	5'-AGGTCGGTGTGAACGGATTTTG-3'
		Reverse	5'-TGTAGACCATGTAGTTGAGGTCA-3'



**Table 2**

List of antibodies used in this study.

<b>Primary Antibody</b>	<b>Supplier</b>	<b>Dilution</b>
Vimentin (AB1620)	Millipore, CA	(1:200)
SOD1 (sc-11407)	Santa Cruz Biotechnology, CA	(1:1000)
Catalase (sc-50508)	Santa Cruz Biotechnology, CA	(1:2000)
NQO1 (ab34173)	Abcam, Cambridge, MA	(1:1000)
NRF2 (ab31163)	Abcam, Cambridge, MA	(1:500)
KEAP1 (sc-15246)	Santa Cruz Biotechnology, CA	(1:800)
HMOX1(AF3776)	R&D Systems, Inc, MN	(1:200)
GPX1(AF3798)	R&D Systems, Inc, MN	(1:100)
GPX2 (MAB5470)	R&D Systems, Inc, MN	(1:200)
GAPDH (MAB374)	EMD Millipore, CA	(1:3000)

<b>Secondary Antibody</b>	<b>Supplier</b>	<b>Dilution</b>
HRP-conjugated anti-rabbit IgG (sc-2004)	Santa Cruz Biotechnology, CA	(1:2000)
HRP-conjugated anti-mouse IgG (sc-2005)	Santa Cruz Biotechnology, CA	(1:2000)
HRP-conjugated anti-goat IgG (sc-2020)	Santa Cruz Biotechnology, CA	(1:2000)
Alexa Fluo 546 anti-rabbit IgG (H+L)	Invitrogen Molecular Probes, NY	(1:1000)
Alexa Fluo 488 anti-rabbit IgG (H+L)	Invitrogen Molecular Probes, NY	(1:1000)
Alexa Fluo 488 anti-goat IgG (H+L)	Invitrogen Molecular Probes, NY	(1:1000)